

All Issues

- Volume 7 | 2025** ▶
- Volume 6 | 2024** ▶
- Volume 5 | 2023** ▶
- Volume 4 | 2022** ▶
- Volume 3 | 2021** ▶
- Volume 2 | 2020** ▶
- Volume 1 | 2019** ▶

Announcements

Great News | Journal of Building Material Science Receives First CiteScore of 0.5!

2025-06-12

Publication Frequency Changed

2025-01-20

Congratulations to Journal of Building Materials Science for being included in Scopus!

2024-12-10

[Show all announcements ...](#)

Indexing



Most Viewed

Concrete Mix Design by IS, ACI and BS Methods: A Comparative Analysis

486

Model-Based Mechanical Property and Structural Failure Prediction of Pseudo Ductile Hybrid Composite

298

Spatial Organisation of Housing and Factors Influencing Residential Choice in the Town of Bol, Lake Province, Chad

236

Compressive Behaviour of

[Home](#) / [Archives](#) / Vol. 7, Iss. 2 (June 2025)



Journal of Building Material Science

ISSN: 2630-5216 (Online)

Vol. 7, Iss. 2 (June 2025)

[← Previous](#)

[Next →](#)

Review

Model-Based Mechanical Property and Structural Failure Prediction of Pseudo Ductile Hybrid Composite

Genetu Amare Dress , Yohannes Regassa , Ermias Gebrekidan Koricho

1-21

Article ID: 8642 DOI: <https://doi.org/10.30564/jbms.v7i2.8642>
 596 (Abstract) 480 (Download)

Abstract: Lightweight fiber reinforced composites are widely used in engineering structures, which often fail catastrophically due to the uncertainty of external loads and their brittle nature. The development of pseudo ductile hybrid composites was the proposed solution to create minimal ductility in fiber reinforced composites so that equipment downtime, cost, and loss of lives can be... [More](#)

PDF

Article

Engineering Design and Construction of Modern Dining Arch

Rabiu Ahmad Abubakar

22-33

Article ID: 8726 DOI: <https://doi.org/10.30564/jbms.v7i2.8726>
 133 (Abstract) 99 (Download)

Abstract: The Building Dining Arch project aimed to create a functional and aesthetically pleasing space that integrated modern architectural design with efficient dining facilities. The structure was conceived to provide a unique dining experience while also serving as a central gathering point for both social and culinary activities. The design incorporated innovative materials and sustainable construction... [More](#)

PDF

Article

Improving the Structural Properties of Sustainable Earthen Construction by Incorporating Lime

Fidjiah Abdelkader , Rabehi Mohamed , Kezrane Cheikh , Deliou Adel , Khemissat Boualem , khorchef mohamed amine

34-46

Article ID: 9115 DOI: <https://doi.org/10.30564/jbms.v7i2.9115>
 161 (Abstract) 82 (Download)

Abstract: Sustainable construction targets the reduction of the negative impacts of construction operations on the environment and improving the utilization of natural resources. It does this by reducing the cost of carbon emissions, the utilization of environmentally friendly materials, reducing energy and water usage, which increases the life of buildings, and reducing wastage through recycling. It... [More](#)

PDF

Article

Effects of Raw Materials, Sintering Conditions, and Stabilizers on High Volume M3-Alite Synthesis

Rajesh Kumar , Shashank Bishnoi , Nagasubramanian Gopalakrishnan

47-57

Article ID: 9181 DOI: <https://doi.org/10.30564/jbms.v7i2.9181>
 99 (Abstract) 55 (Download)

Reinforced Concrete Columns
Using Recycled Building Glass
Instead of Sand Aggregate in
Concrete

223

Effect of Crystalline Admixture on
the Mechanical and Durability
Properties of M40 Grade of
Concrete

202

Abstract: The study presents the process to synthesize and characterize the M3 polymorph of Tricalcium oxy silicate, also known as alite ($\text{Ca}_3\text{O}(\text{SiO}_4)$), a major component in Portland cement. An optimized solid-state reaction protocol has been established for synthesizing high volume pure M3-alite. The effects of raw materials, sintering conditions, degree of compaction, and stabilizers were studied on the... [More](#)

PDF

Article

Spatial Organisation of Housing and Factors Influencing Residential Choice in the Town of Bol, Lake Province, Chad

Parfait Altolnan Tombar [ID](#), Abdou Kailou Djibo [ID](#), Vidjinnagni Vinasse Ametooyona Azagoun [ID](#), François Teadoum Naringué [ID](#), Emmanuel Loumouna [ID](#), Komi Selom Klassou [ID](#)

58-79

Article ID: 9374 DOI: <https://doi.org/10.30564/jbms.v7i2.9374>
236 (Abstract) 62 (Download)

Abstract: Housing, access to which is recognised as a universal right for all, embodies the values, traditions and social dynamics specific to different communities. It is a place of residence whose choice is often influenced by social, economic, religious, demographic, cultural and environmental factors. The housing in Bol, a Sahelian town in the Lac province of... [More](#)

PDF

Review

Light Transmitting Concrete: A State-of-the-Art Review on Performance and Potential

Kaushal Sharma [ID](#), Kiran Devi [ID](#), Neeraj Saini [ID](#)

80-96

Article ID: 9578 DOI: <https://doi.org/10.30564/jbms.v7i2.9578>
111 (Abstract) 46 (Download)

Abstract: The use of artificial lighting, particularly in urban areas, contributes to global warming and carbon footprints. Urban expansion is unregulated and unplanned in emerging nations. In the case of India, the urban community is the major consumer of electric power. The invention of Light-transmitting concrete (LTC) lets light pass through opaque concrete and lowers the... [More](#)

PDF

Article

Effect of Diameter and Number of Bolts on the Rotation Stiffness of Beam-to-Column Timber Joints

Yosafat Aji Pranata [ID](#), Olga Catherina Pattipawaej [ID](#), Amos Setiadi [ID](#)

97-110

Article ID: 9704 DOI: <https://doi.org/10.30564/jbms.v7i2.9704>
116 (Abstract) 77 (Download)

Abstract: Beam-to-column joints affect the behavior of the building. This research aims to obtain an empirical equation of the rotational stiffness of the beam-to-column timber joints with variations in the number and diameter of bolts. The method used is the destructive method to obtain elastic and post-elastic history of load and deformation of timber joints. The... [More](#)

PDF

Article

Influence of Fly Ash, Alcofine, Alkaline Molarity, Curing Duration and Machine Learning Predictions on Geopolymer Concrete

Sayali A. Baitule [ID](#), Bhushan H. Shinde [ID](#)

111-121

Article ID: 9693 DOI: <https://doi.org/10.30564/jbms.v7i2.9693>
87 (Abstract) 43 (Download)

Abstract: The study is motivated from the perspective of developing an eco-friendly and effective alternative to cement-based materials. One of the contributions of this research lies in the assessment of three different concentrations of sodium hydroxide (8M, 12M, and 16M) along with the use of Activated Low-Calcium Fly Ash (ALF) as a supplementary cementitious material. Another... [More](#)

PDF

Article

Mechanical Performance of Fiber-Reinforced Self-Compacting Concrete: Comparative Analysis and Structural Implications

Hemant B Dahake [ID](#), Bhushan H Shinde [ID](#)

122-135

Article ID: 9694 DOI: <https://doi.org/10.30564/jbms.v7i2.9694>
64 (Abstract) 44 (Download)

Abstract: The aim of this study is to assess the mechanical properties of different types of fibre-reinforced self-compacting concrete (FRSCC) such as steel fibre (SFSCC), glass fibre (GFSCC), polypropylene fibre (PFSCC) and plain self-compacting concrete (SCC). This will involve the evaluation of various fibres' influences on the key strength parameters including compressive, split tensile, flexural and... [More](#)

PDF



Article

Experimental Study on the Influence of TiO₂ and GGBS on Concrete Durability and Impact Strength

Mamidi Srinivasan , Pothukuchi Sravana 

136-152

Article ID: 9695 DOI: <https://doi.org/10.30564/jbms.v7i2.9695>

 116 (Abstract)  58 (Download)

Abstract: The paper examines the improvements in M40 and M50 grade concrete properties resulting from adding nano-titania and using ground granulated blast-furnace slag as a replacement for cement in an effort to produce an environmentally friendly concrete substitute. The concrete mixes were formulated by following IS 10262:2019 and the different mix combinations comprised 0.5% to 2%... [More](#)

 PDF



Article

A Study on Factors Influencing Cost Management in Green Building Construction

MingQi Yang

153-174

Article ID: 9770 DOI: <https://doi.org/10.30564/jbms.v7i2.9770>

 134 (Abstract)  67 (Download)

Abstract: Green buildings represent a crucial solution for reducing carbon emissions in the construction sector, which accounts for approximately one-third of global energy-related emissions. However, high initial costs remain a significant barrier to widespread adoption of sustainable construction practices. This study addresses the critical gap in understanding how cost factors interconnect throughout the entire lifecycle of... [More](#)

 PDF



Article

Utilizing Nano-TiO₂ and GGBS to Improve Concrete's Acid Resistance and Durability

Mamidi Srinivasan , P. Sravana 

175-192

Article ID: 9696 DOI: <https://doi.org/10.30564/jbms.v7i2.9696>

 111 (Abstract)  54 (Download)

Abstract: Although concrete is a commonly used building material, it suffers deterioration in acidic surroundings. Significant structural damage and expensive repairs can follow from this. This work examined the strength and durability of M40 and M50 grade concrete incorporating 30% ground granulated blast furnace slag (GGBS) and 1% titanium dioxide (TiO₂). Several tests, including an acid... [More](#)

 PDF



Article

Reutilization Potential of Fine Fraction from Construction and Demolition Waste in the Circular Economy

Ville Lahtela , Ida Rasilainen , Timo Kärki 

193-203

Article ID: 9786 DOI: <https://doi.org/10.30564/jbms.v7i2.9786>

 129 (Abstract)  42 (Download)

Abstract: Fine fraction waste is a remarkable secondary material without a rational utilization objective, demonstrating a real research gap for its study. The fine fraction can constitute up to several dozen percent of the total waste volume, representing a significant amount of material, but the nature of material can be partly complex and heterogeneous, restricting its... [More](#)

 PDF

About Us

- Profile
- Payment Collection Information
- Contact and support

Further Information

- All Journals
- Other Journals

Follow Us



Facebook



Twitter



LinkedIn



YouTube



ARTICLE

Effect of Diameter and Number of Bolts on the Rotation Stiffness of Beam-to-Column Timber Joints

Yosafat Aji Pranata^{1*}, Olga Catherina Pattipawaej², Amos Setiadi³

¹Master Program in Civil Engineering, Maranatha Christian University, Bandung 40164, Indonesia

²Bachelor Program in Civil Engineering, Maranatha Christian University, Bandung 40164, Indonesia

³Doctoral Program in Architecture, University of Atma Jaya Yogyakarta, Sleman 55281, Indonesia

ABSTRACT

Beam-to-column joints affect the behavior of the building. This research aims to obtain an empirical equation of the rotational stiffness of the beam-to-column timber joints with variations in the number and diameter of bolts. The method used is the destructive method to obtain elastic and post-elastic history of load and deformation of timber joints. The scope of the research is the timber using red meranti (*Shorea* spp.) species, with a cross-sectional size of 50mm x 100mm, bolts using various diameters of 8, 10, and 12mm. Beam-to-column timber joints use a variety of one, two, and three bolts. Testing uses a monotonic loading type. The behaviors reviewed are load-carrying capacity and rotational stiffness. The results obtained from this research, which are the proposed bilinear moment-rotational stiffness relationship curve model for beam-to-column timber joints, can provide benefits in modeling and analyzing the structure of multi-storey wooden buildings, especially in modeling parameters of spring elements for beam-to-column joints of red meranti (*Shorea* spp.) timber. The proposed equation for moment capacity and rotational stiffness in terms of elastic range, namely M_y and θ_y , has an R^2 of 0.86 and 0.87, respectively. These results indicate a strong relationship between moment capacity, bolt diameter size, and number of bolt variables in a statistical model. In the design context, the parameters used are at elastic limit range conditions. The results of the research show that the number of bolts has a significant effect on the beam-to-column joint, namely the non-linear moment and rotational capacity increases.

Keywords: Moment Capacity; Rotation Stiffness; Beam-To-Column; Timber; Ductile

*CORRESPONDING AUTHOR:

Yosafat Aji Pranata, Master Program in Civil Engineering, Maranatha Christian University, Bandung 40164, Indonesia; Email: yosafat.ap@maranatha.ac.id

ARTICLE INFO

Received: 25 April 2025 | Revised: 20 May 2025 | Accepted: 23 May 2025 | Published Online: 6 June 2025

DOI: <https://doi.org/10.30564/jbms.v7i2.9704>

CITATION

Pranata, Y.A., Pattipawaej, O.C., Setiadi, A., 2025. Effect of Diameter and Number of Bolts on the Rotation Stiffness of Beam-to-Column Timber Joints. *Journal of Building Material Science*. 7(2): 97–110. DOI: <https://doi.org/10.30564/jbms.v7i2.9704>

COPYRIGHT

Copyright © 2025 by the author(s). Published by Bilingual Publishing Group. This is an open access article under the Creative Commons Attribution-NonCommercial 4.0 International (CC BY-NC 4.0) License (<https://creativecommons.org/licenses/by-nc/4.0/>).

1. Introduction

A timber-framed building is a structure constructed with a strong, visible framework of large timbers joined together with traditional methods like mortise and tenon joinery. A multi-storey timber building with a frame structure system is a building with main structural components^[1], consisting of columns and beams using a beam-column joint system. Timbers are joined with precise fitting. Beam-to-column joints, especially in timber buildings with moment-resisting frame systems are the main parameters of structural rigidity and strength under gravitational and lateral loading such as earthquake loads.

The connection system affects both the behavior of the building globally and locally (joints). Experimental tests and numerical analysis of the moment-resisting frame beam-to-column timber joints have recently been carried out to evaluate the strength and stiffness capabilities. In numerical modeling of multi-storey wooden frame buildings, modeling of structural elements and connections affects the results of the overall structural analysis of the building^[2-4]. Connection modeling in this context is the rotational stiffness and load-carrying capacity parameters^[5]. The beam-to-column timber joints are neither pinned nor rigid, but their rotational stiffness is in the range of the two types. An understanding of the behavior of beam-to-column timber joint connections is required, which are the moment and the rotation in terms of yield and ultimate loads.

The research question is whether parameters, such as moment-carrying capacity, rotational capacity, and ratio of ductility of the joints increase with increasing the number of bolts and enlarging bolt diameter. The hypothesis in this study is that adding mechanical connectors and steel plates that are a stiffer and more ductile material to beam-to-column timber connection results in joints with better performance, in terms of parameters described previously.

This research aims to obtain an empirical equation of the rotational stiffness of the beam-to-column timber joints with variations in the number and diameter of bolts.

The method used in this research is the destructive method of obtaining elastic and post-elastic history of load and deformation of timber joints. The experimental test is used to obtain the empirical data of moment capacity and rotational stiffness of the beam-to-column timber joints. To

determine the parameter of rotational stiffness, it is necessary to determine the displacement of the beam member. The displacement sensors were mounted on the point load that applied to the beam member of the specimens. The scope of the research is the beam-to-column timber joints using the red meranti (*Shorea* spp.) species with a cross-sectional size of 50 mm × 100 mm, bolts using various diameters of 8mm, 10mm and 12mm. Beam-to-column timber joints use a variety of one, two, and three numbers of bolts. The joints use 5mm-thick steel side plates (double steel plates). Each type of joint uses 1 specimen, so there are a total of 9 (nine) specimens. Testing uses a destructive method with the Universal Testing Machine instrument to obtain a load and deformation curve. The test uses a monotonic loading type. The behaviors reviewed are strength capacity and rotational stiffness. **Figure 1** shows the flowcharts of this study.

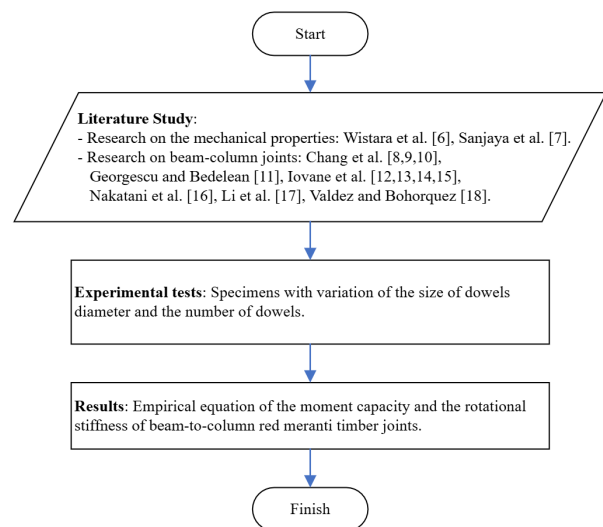


Figure 1. The Flowcharts of This Study^[6-18].

Red meranti is a fast-growing species^[6]. In Indonesia, the growth rate of red meranti timber has been intensively carried out through a system of selective cutting and line planting silviculture^[7].

Research on wooden beam and column connections has been conducted by several researchers, with the aim of investigating the strength and stiffness behavior of the connection. Chang et al. have conducted experimental tests on the beam-to-column joints of the Taiwan and Japan timber frame structures^[8], which are similar in appearance. The parameter studied is the rotational performance of traditional timber joints. Chang and Hsu continue the research

by proposing a theoretical model to calculate the behavior of beam-to-column joints of timber frame structures^[9]. Chang and Hsu continue the research by conducting the destructive experimental test of full-scale beam-to-column timber specimens^[10]. The type of loading is cyclic to obtain the hysteretic loop of the joints.

Georgescu and Bedeleian have conducted research with the objective of learning the effect of depth of dowel embedment, dowel spacing, and length of dowel on the timber joints made of ash (*Fraxinus excelsior*) timber^[11]. The results obtained from the research were that the strength of joints increases when the length of dowel increases, the dowel spacing increases, and the ratio of dowel embedment decreases.

Iovane and Faggiano have researched a numerical investigation, and continue with an experimental test on the beam-to-column of a timber joint using a steel link as a connector^[12,13], with the results obtained from an experimental indicate a good agreement with the prediction that calculated using theoretical equation. The research was then developed into a proposal for the analysis and design of dissipative seismic-resistant timber structures using steel links^[14]. Iovane et al. have also researched and proposed a procedure for the classification of beam-to-column joints using mechanical connectors, with behavior reviewed by strength and stiffness in timber buildings^[15].

A study on the beam-column joint of timber frame structures using mechanical fasteners and special connectors has been conducted by Nakatani et al.^[16], the joints use a steel plate and a special connector to increase the ductility and to prevent the joints from failure. Li et al. have conducted an investigation into the rotational behavior of beam-to-column timber joints as a partial component of the beams and columns in timber frames^[17], to study the effect of rotational stiffness in terms of perpendicular to the grain on the rotational behavior of joints. Valdez and Bohorquez conducted research to investigate and explore the optimization of bio-based sewing timber joints^[18].

mented by partial or physical testing of structure members and connections, it is now possible to design and optimize the timber building^[19]. A beam to column joints is a structural joint that links a beam and a column, typically used in buildings to transfer loads from the beam to the column. These connections are crucial for the stability and load-bearing capacity of the structure, and can be designed in various ways depending on the materials used and the structural requirements. Beam-to-column timber joints connect beams and columns members in wooden structures, and their design significantly impacts the strength and stiffness of the building. These connections can be all-timber, utilize metal fasteners. Key aspects of beam-to-column timber joints include their ability to transfer moments, and shear forces.

Beam-to-column joints can be classified into three different methods of structural analysis. The first method is elastic analysis, using the linear moment and rotational stiffness parameters. The second method is rigid-plastic analysis, using the assumption that the yield and ultimate moments are in terms of equal values, but they have different values between yield rotation and ultimate rotation. The last method is an elastic-plastic analysis, using the yield and ultimate moments and rotational stiffness parameters, provided that the idealized curve of moment-rotational stiffness can be developed based on a bilinear model^[15]. The general idealization curve model is used for stress-strain modeling of reinforcing steel as well, to model the material conditions in the elastic and post-elastic ranges^[20].

The moment at the yield or proportional point condition (M_y) is calculated using Equation 1 (yielding moment) and the ultimate condition (M_u) is calculated using Equation 2 (ultimate moment). The rotation at the proportional point condition (θ_y) is calculated using Equation 3, and the ultimate condition (θ_u) is calculated using Equation 4. The ratio of ductility of joints (μ) can be calculated using Equation 5.

$$M_y = P_y \cdot 900 \quad (1)$$

$$M_u = P_u \cdot 9000 \quad (2)$$

$$\theta_y = \Delta_y / 900 \quad (3)$$

$$\theta_u = \Delta_u / 900 \quad (4)$$

2. Theoretical Background

2.1. Beam-to-Column Joints

Wood is an orthotropic material. With the development of connections and numerical simulations supple-

$$\mu = \Delta_u / \Delta_y \quad (5)$$

where P_y is yield load (N), P_u is ultimate load (N), M_y is moment in term of yield load (N.mm), and M_u is moment in term of ultimate load (N.mm), Δ_y is deformation in term of yield load (mm), Δ_u is deformation in term of ultimate load (mm), θ_y is rotation in term of yield load (mm), θ_u is rotation in term of ultimate load (mm), and μ is ratio of ductility (mm/mm). The value of 900 (unit length in millimeters) in Equations 1 to 4 is the distance between the load and the center of the beam-to-column joint, as shown in **Figure 2**. Equation (5) is used to calculate the ratio of ductility of joints ^[21].

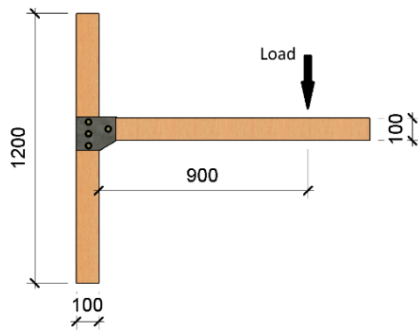


Figure 2. Schematic Illustration of the Beam-To-Column Joint Specimen (Unit Length in Millimeters).

2.2. Determining the Yield Points

To investigate the post-elastic behavior of beam-to-column joints, it is important to know the proportional point, which is the condition of the behavior of joints changed from elastic to plastic. Some methods can be used to determine the proportional points. One of the methods to determine the proportional load and deformation is proposed by The Commonwealth Scientific and Industrial Research Organization ^[22].

The Commonwealth Scientific and Industrial Research Organization has developed a method to determine the yield or proportional point ^[22]. This method for determining the yield point of timber defines it as the point on the load-deformation curve where the deformation is 1.25 times the deformation at 40% of the maximum capacity. This is a practical approach for identifying the point where the timber transitions from elastic to plastic behavior.

The method first identifies the deformation that corresponds to 40% of the timber's maximum load-carrying

capacity. The proportional point (Δ_y) can be calculated using Equation 6, which is obtained by multiplying the value of the deformation at 0.4 of the ultimate or peak load by a factor of 1.25 as shown in **Figure 3**. The point on the curve of load versus deformation is formed by the intersection of the projected line from the new factored deformation point, which is then taken as the proportional or yield point, so the corresponding yield load (P_y) is determined.

$$\Delta_y = 1.25\Delta_{0.4} \quad (6)$$

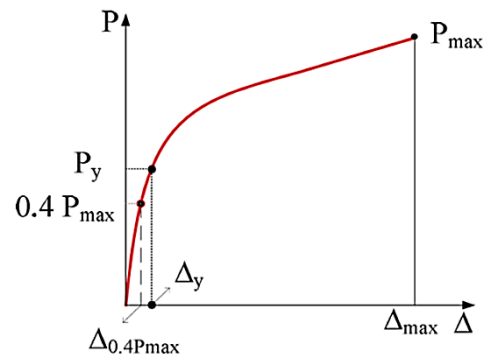


Figure 3. Method to Determine Yield (Proportional) Point Using CSIRO Method ^[22].

2.3. Multiple Regression Analysis

Regression analysis is a statistical method that can be used to develop the equation to present the relationships between a dependent variable and one or more independent variables. Multiple regression analysis is a statistical procedure to calculate the value of a response variable as a dependent variable from the value of the independent predictor variable ^[23]. The multiple linear regression equation is given by Equation (7).

$$y = a + b_1x_1 + \dots + b_nx_n \quad (7)$$

where x_n is independent variables and y is dependent variable.

The aim of the multiple regression is to describe and understand the relationship, to predict a new observation, and to adjust and control a process ^[24]. The objective of multiple regression analysis is to model the relationship between a dependent variable and one or more independent variables. When the number of independent variables increases, it will create changes within dependent factors. Key aspects of multiple regression are the variable being predicted, which must be continuous. The method assumes

a linear relationship between the dependent and independent variables, though this can be relaxed with non-linear regression techniques.

3. Methods

In this study, a destructive method was used to obtain the load history curve versus the deformation of the beam-to-column joint. With the destructive method, the maximum capacity of the connection can be determined and the failure pattern that occurs in the connection can be studied. **Table 1** and **Figure 4** show the types of specimens that were used in the study.

The dimensions of the beam and column are 50 mm × 100 mm. Beam-to-column joints use variations in the number and size of bolts; one specimen for each type, and the total is nine specimens. Bolts use a variety of diameter sizes of 8 mm, 10 mm, and 12 mm. The number of bolts uses variations of one bolt, two bolts, and three bolts. **Figure 4a** shows a beam-to-column joint with one bolt, **Figure 4b** shows a beam-to-column joint with two bolts using a 50 mm length of bolt spacing, and **Figure 4c** shows a beam-

to-column joint with three bolts using a 50 mm length of each bolt's space. The distance between bolts in one row is 50 mm. This does not exceed the minimum spacing rule between bolts in the Indonesian wood code SNI 7973 ^[25].

The bolt tightening method used in this study is the snug tight method. In AISC specifications ^[26], a snug tight bolted connection is achieved when all plies are pulled into firm contact, and the bolts are tightened enough to prevent the removal of the nuts without a wrench. This research on beam-to-column joints uses mechanical connectors, which are bolts and steel plates, so that failure is not expected to occur in bolts or steel plates. Therefore, a mechanical property test was first carried out, namely a tensile test to determine the tensile strength of the steel plate and the bolts used as connectors.

Tensile tests of steel plates were carried out to obtain tensile yield strength (F_y) and tensile strength (F_u). The tests were in accordance with ASTM E8/E8M-22 ^[27], with the specimen type being flat, gauge length is 200mm. The method of testing is based on the control of the strain speed, which is 0.015mm/mm/minute.

Table 1. The Type of the Specimen.

No	Specimen's Name	Diameter of Bolt (mm)	Number of Bolt	Steel Plate Thickness (mm)	Number of Specimen
1	BCJ.8.1	8	1	5	1
2	BCJ.8.2	8	2	5	1
3	BCJ.8.3	8	3	5	1
4	BCJ.10.1	10	1	5	1
5	BCJ.10.2	10	2	5	1
6	BCJ.10.3	10	3	5	1
7	BCJ.12.1	12	1	5	1
8	BCJ.12.2	12	2	5	1
9	BCJ.12.3	12	3	5	1

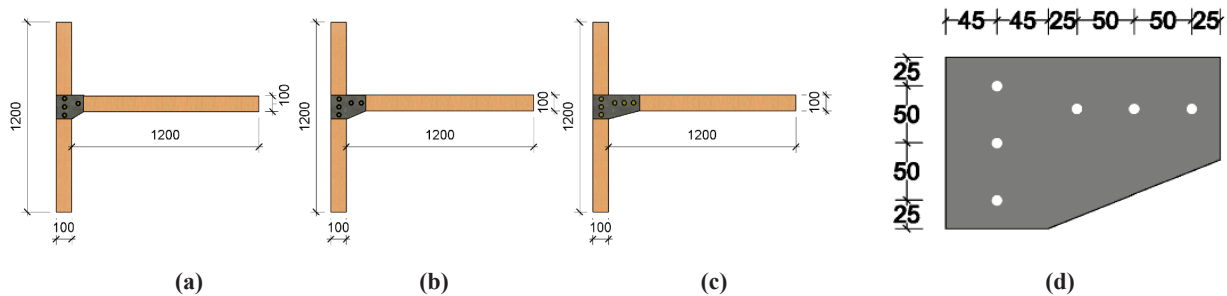


Figure 4. The Types of Specimens That Used in the Study. (a). Specimen with One Bolt. (b). Specimen with Two Bolts. (c). Specimen with Three Bolts. (d). Details of Bolt Spacing (50 mm), End Distance (25 mm), and Edge Distance (25 mm) for a Specimen with Three Bolts (Units in Millimeters).

Tensile tests of bolts were also carried out to obtain the yield stress and tensile strength. The tests conform to ASTM F606/F606M^[28]. The method of testing is based on the control of the displacement speed, which is 3.0 mm/minute.

4. Results

The test results of steel plates that are used for side members of beam-column joints for all the specimens are shown in **Figure 5** (tensile tests), Specimen S5-1 (**Fig-**

ure 5a), Specimen S5-2 (**Figure 5b**), and Specimen S5-3 (**Figure 5c**), respectively. **Figure 6** shows the stress-strain relationships obtained from tensile tests of steel plates that used for side members of the joints. **Table 2** shows the yield strength and the ultimate strength of the steel plates obtained from tensile tests. As seen in **Table 2**, the results of the steel tensile tests showed that the tensile yield stress and tensile strength stresses are 318.13 MPa and 421.76 MPa, respectively. The failure mode of all the specimens was fracture of the rod that was the object of the tensile test.

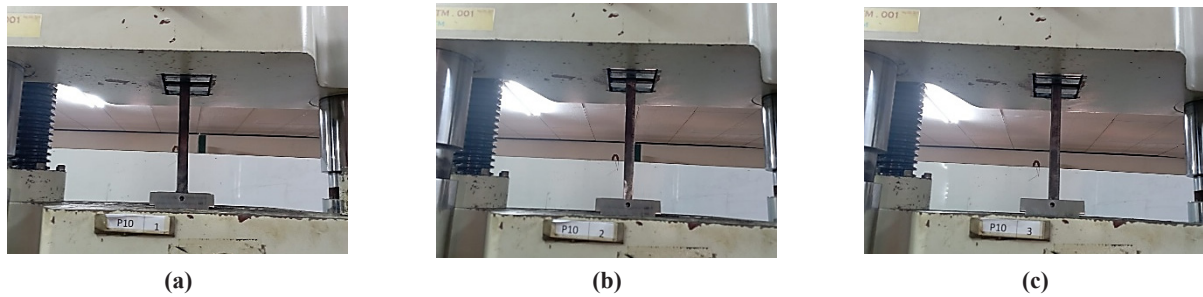


Figure 5. Tensile Tests of the Steel Plates. (a). Specimen S5-1. (b). Specimen S5-2. (c). Specimen S5-3.

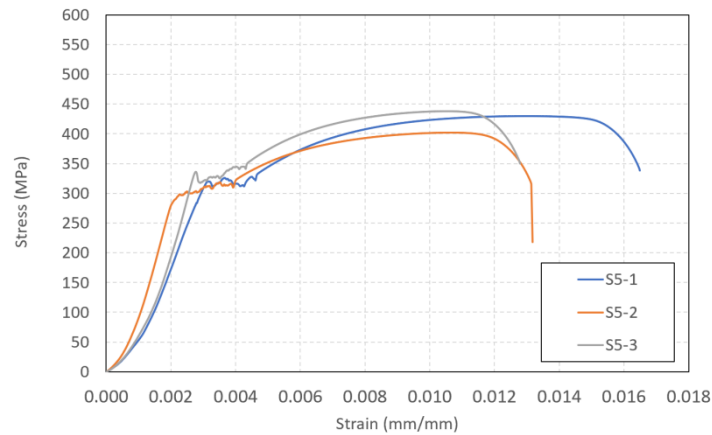


Figure 6. Stress-Strain Curves Obtained from Tensile Tests of Steel Plates.

Table 2. Results Obtained from Tensile Tests of Steel Plates.

Specimen	P_y (N)	F_y (MPa)	P_u (N)	F_u (MPa)	Specimen
S5-1	56714.14	318.04	76206.96	427.35	S5-1
S5-2	53557.95	302.07	71347.75	402.41	S5-2
S5-3	59653.01	334.29	77717.28	435.52	S5-3
Average	56641.70	318.13	75090.66	421.76	Average

The tensile strength and yield bending strength of bolts tend to have a decreasing trend due to the influence of the increasing diameter size ^[29,30]. Therefore, in this study, the diameter of the bolts used is limited to the largest diameter, which is 12 mm. Experimental research to determine the mechanical properties of bolts, namely tensile strength (F_y) has been conducted previously. The results of the research showed that the tensile strength (F_y) of 8mm diameter bolts was obtained at 716.60 MPa, while for 10 mm diameter bolts it was 529.62 MPa ^[29]. The minimum yield strength of the bolt according to ASTM A307-21 is 413 MPa ^[31].

The complete test results of the 12mm diameter bolts that are used as the highest diameter fasteners of beam-column joints are shown in **Figure 7** and **Table 3**. **Figure 7a** shows the tensile test. The failure mode of all the specimens was that the bolt broke at the area of gauge length (**Figure 7b**). As seen in **Table 3**, the bolt yield stress and tensile strength are 354.54 MPa and 388.47 MPa, respectively.

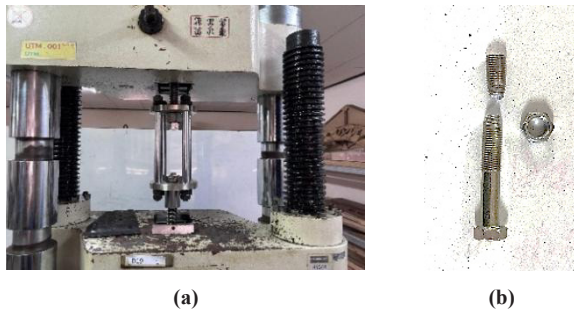


Figure 7. Tensile Tests of 12-mm Diameter Bolts. (a) Tensile Test. (b) Failure of the Specimen.

Table 3. Results Obtained from Tensile Tests of 12-mm Diameter Bolts.

Specimen	P_y (N)	F_y (MPa)	P_u (N)	F_u (MPa)	Specimen
B12-1	33375.78	351.06	37056.94	389.78	B12-1
B12-2	34409.20	361.93	39858.70	419.25	B12-2
B12-3	33335.37	350.64	33882.03	356.39	B12-3
Average	33706.78	354.54	36932.56	388.47	Average

Furthermore, testing of the beam-column joints uses a destructive method with the Universal Testing Machine

(UTM) instrument HT-9501 to obtain a load vs deformation history curve ^[32]. The test uses a monotonic loading type, by placing the load cell of 1000 kN at the near-end of the beam. Displacement measurement using a transducer located on the UTM. The UTM records changes in the distance of the load block, so that it is recorded as a history of the displacement curve.

The distance from the center of the beam-to-column joint axis to the load is 900 mm as shown in **Figure 2**. The support model at the ends of the column (top and bottom) is a pin-support type. The methods were displacement controlled at a speed of 2.5 mm/min. The location of the load placement is as shown in **Figure 2**. At that point, a load with a gradually increasing value is applied in the form of constant displacement.

As presented in **Figure 8**, **Figure 8a** shows the setup of the 8mm beam-to-column specimen on Universal Testing Machine, **Figure 8b** shows testing of the specimen, and **Figure 8c** shows the shape of the specimen after testing. In **Figure 9**, **Figure 9a** shows the setup of the 10 mm beam-to-column specimen on Universal Testing Machine, **Figure 9b** shows testing of the specimen, and **Figure 9c** shows the shape of the specimen after testing. In **Figure 10**, **Figure 10a,b** show examples of two 12 mm beam-to-column specimens and **Figure 10c** shows testing of the specimen.

Figure 11 shows a failure pattern from some specimens. **Figure 11a** shows the failure pattern of a single 8mm bolt of beam-to-column specimen. The failure occurred in the bolt hole. This condition indicated indicates that was the bearing failure. **Figure 11b** and **Figure 11c** show the failure pattern of two 10mm bolts and single 12mm bolts of beam-column-specimens, where similar occurred in the bolt's holes. The failure mode, as shown in **Figure 11**, occurs because the bearing strength of the timber has been exceeded due to contact with the bolt. The bearing strength of red meranti wood, which is 32.74 MPa ^[33], is much lower than the bolt capacity as shown in the test results shown in **Table 3**.

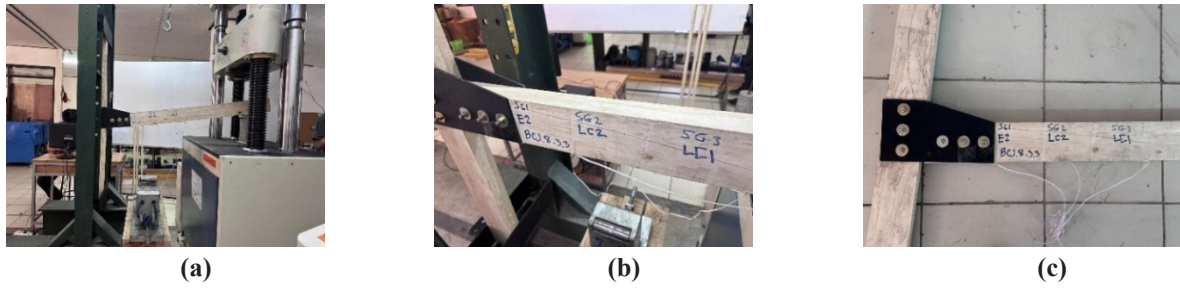


Figure 8. Setup, Testing, and Post-Test of the Beam-To-Column Specimens Using 8 mm Diameter of Bolt. (a) Setup of the Specimen. (b) Testing of the Specimen. (c) Post Test of the Specimen.

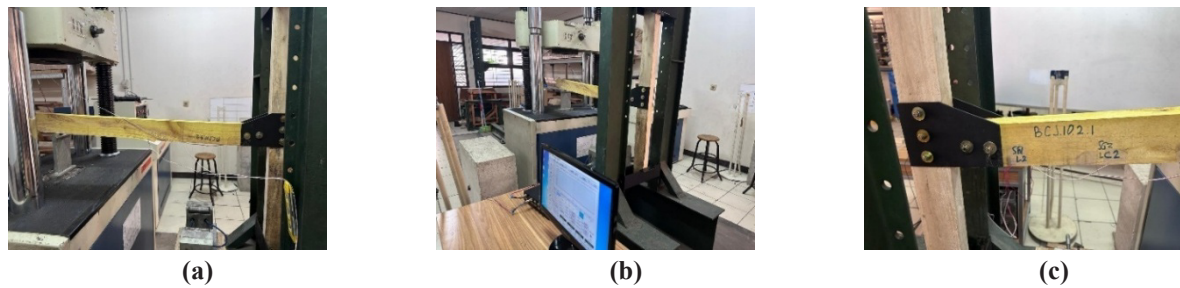


Figure 9. Setup, Testing, and Post-Test of the Beam-To-Column Specimens Using 10 mm Diameter of Bolt. (a) Setup of the Specimen. (b) Testing of the Specimen. (c) Post Test of the Specimen.

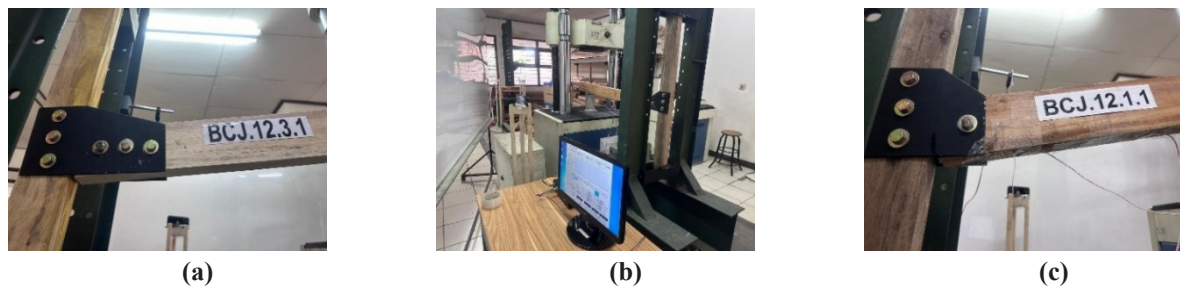


Figure 10. Setup, Testing, and Post-Test of the Beam-To-Column Specimens Using 12 mm Diameter of Bolt. (a) Setup of the Specimen. (b) Testing of the Specimen. (c) Post Test of the Specimen.

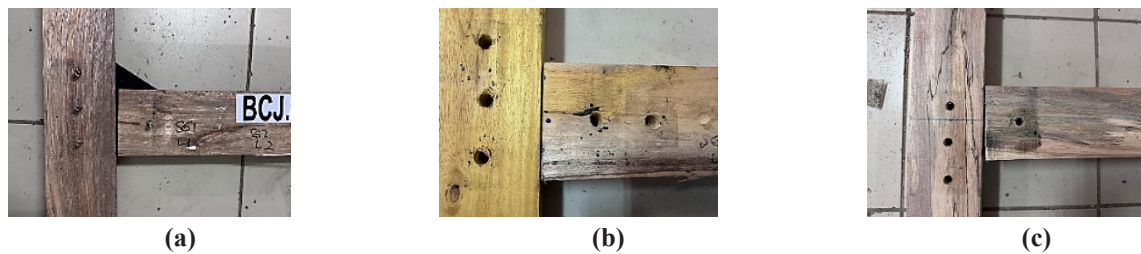


Figure 11. Failure Patterns of the Beam-To-Column Joint Specimens Using 12 mm Bolts. (a) Specimen Using 8 mm Bolts. (b) Specimen Using 10mm Bolts. (c) Specimen Using 12 mm Bolts.

The load and deformation relationship curves of the experimental test results are shown in **Figure 12** for connections with 8mm-diameter bolts, **Figure 13** for connections with 10mm-diameter bolts, and **Figure 14** for connections with 12mm-diameter bolts. In general, from **Figures 12** to **14**, it can be seen that the trend of the load and deformation relationship curves has a bilinear pattern. Namely, in the initial loading range, the condition of the connection still behaves elastically until the proportional point (yield) is reached. After that, the connection behaves post-elastically until it reaches the ultimate load and failure occurs.

As seen in **Figures 12** and **13**, the curves for BCJ.8.2.1 and BCJ.10.3.1 specimens display unexpectedly similar behavior and both show an inverse peak post-yield, despite differing bolt diameters and quantities. This is because in these specimens there is a failure of the bolthole (bearing capacity) on the beam, namely the bolt at the end. After the hole fails, a split mechanism occurs in the direction parallel to the wood grain. However, the connection system can still withstand the load, so that there is a trend of a sharp decrease in load capacity, then an increase again. The cause of this phenomenon in both test specimens could be due to the influence of homogeneity in the non-uniform wood material.

Table 4 shows the yield loads (P_y) and yield deformations (Δ_y) obtained using the CSIRO method ^[22] and deformation in terms of yield point, the ultimate loads (P_u) and deformations (Δ_u), while **Table 5** shows the calculation of moments (M) and rotations (θ). The calculation results of the ratio of ductility of joints in **Table 4** show that the beam-to-column joint with a single bolt of 8mm diameter (Specimen BCJ.8.1.1) produces a high ductility ratio, as a consequence of the joint behaving like a pin, namely a limited load-carrying capacity of 113.2 N (proportional limit condition), after which the joint behaves inelastically until it fails. Similar conditions also occur in Specimen BCJ.10.1.1, namely a single bolt connection with a diameter of 10mm. The single-bolt connection with a diameter of 12mm (BCJ.12.1.1) shows a significantly increased load-carrying capacity value, which is 2.03 times higher than BCJ.8.1.1, because the cross-sectional area of the bolt is indeed 2.25 times higher. While BCJ.12.1.1 has a load-carrying capacity of 1.52 times higher than BCJ10.1.1

because the cross-sectional area of the bolt is indeed 1.44 times higher.

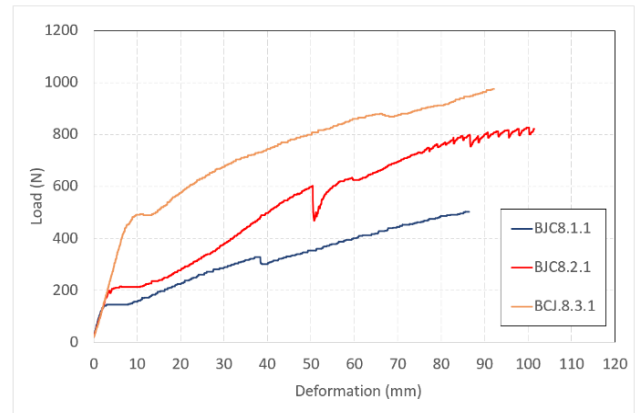


Figure 12. Load Versus Displacement Curves Obtained from Tests, the Specimen Using 8mm Bolts.

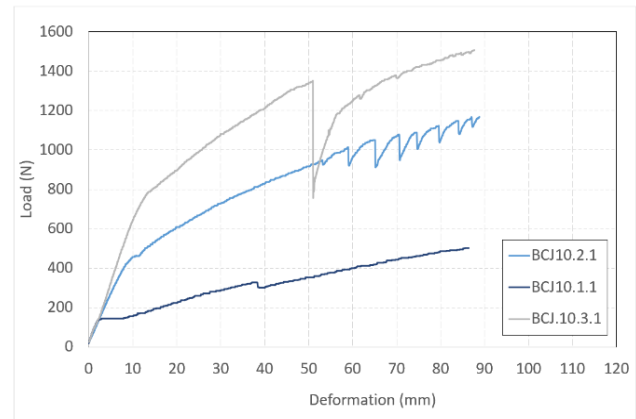


Figure 13. Load Versus Displacement Curves Obtained from Tests, the Specimen Using 10mm Bolts.

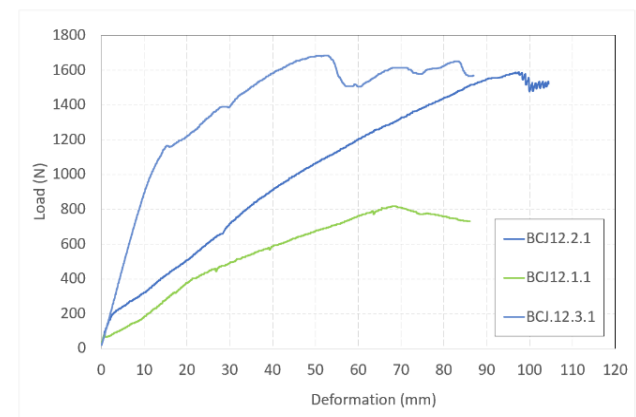


Figure 14. Load Versus Displacement Curves Obtained from Tests, the Specimen Using 12mm Bolts.

Table 4. Results Obtained from Tests: Load-Carrying Capacity, Deformation, and Ratio of Ductility.

Specimen	P_y (N)	Δ_y (mm)	P_u (N)	Δ_u (mm)	μ
BCJ.8.1.1	113.2	1.7	502.4	86.4	50.8
BCJ.8.2.1	194.6	3.1	821.5	99.5	32.1
BCJ.8.3.1	454.9	8.0	970.9	91.4	11.4
BCJ.10.1.1	151.6	2.4	500.1	85.4	35.6
BCJ.10.2.1	384.7	7.5	1158.7	88.2	11.8
BCJ.10.3.1	733.2	12.0	1505.0	87.6	7.3
BCJ.12.1.1	230.9	12.9	810.4	69.2	5.4
BCJ.12.2.1	441.3	16.1	1581.9	97.6	6.1
BCJ.12.3.1	1147.4	14.8	1661.1	81.5	5.5

Table 5. The Moment and Rotational Parameters Calculation.

Specimen	M_y (N.mm)	M_u (N.mm)	θ_y (rad.)	θ_u (rad.)	Specimen
BCJ.8.1.1	101,880	452,160	0.002	0.096	BCJ.8.1.1
BCJ.8.2.1	175,140	739,350	0.003	0.111	BCJ.8.2.1
BCJ.8.3.1	409,410	873,810	0.009	0.102	BCJ.8.3.1
BCJ.10.1.1	136,440	450,090	0.003	0.095	BCJ.10.1.1
BCJ.10.2.1	346,230	1,042,830	0.008	0.098	BCJ.10.2.1
BCJ.10.3.1	659,880	1,354,500	0.013	0.097	BCJ.10.3.1
BCJ.12.1.1	207,810	729,360	0.014	0.077	BCJ.12.1.1
BCJ.12.2.1	397,170	1,423,710	0.018	0.108	BCJ.12.2.1
BCJ.12.3.1	1,032,660	1,494,990	0.016	0.091	BCJ.12.3.1

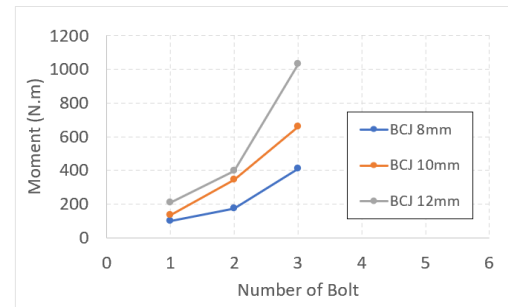
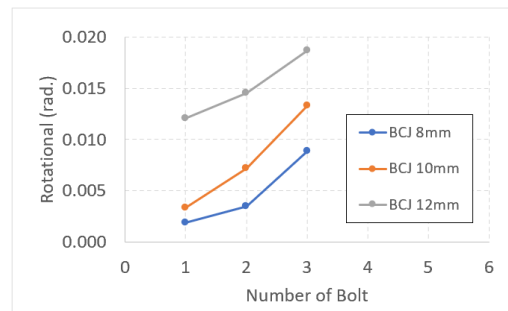
Table 5 shows the results of moment and rotation calculations under proportional limit load and ultimate limit load conditions. The moment and stiffness relationship curve model is an important parameter in modeling the rotational stiffness of beam-to-column joints for modeling and analyzing frame-type wooden building structures, which is usually carried out to study the strength and stiffness behavior of wooden buildings. The bilinear curve model with ductile trend is a curve model that shows good stiffness behavior for wood joints, because it provides a general ductile behavior impact for wood structures with frame systems.

The ratio of ductility is the structure's ability to be have large deformations in the post-elastic range without a substantial reduction in load-carrying capacity^[34,35]. In moment-resisting timber frame systems, the ratio of ductility is mainly achieved through the beam-to-column joints. Eurocode 8 states that structural members must behave linearly and that all non-linear behavior must be concentrated on the beam-to-column joints^[36]. In other words, the ratio of ductility is measured by the ratio between the peak de-

formation and the deformation at the end of elastic range.

4. Discussion

The calculation results as shown in **Table 3**, **Figure 15**, and **Figure 16**, showing that the moment and rotation capacity increases with the increase in the number of bolts, both for specimens using 8mm, 10mm and 12mm bolts. However, the addition of bolts has the effect of reducing the displacement-ductility of the beam-to-column joints. This is influenced by the bolt group action factor^[25,37]. The group action factor describes the effect of the number of mechanical connectors in a row on the normalized capacity of the joints.

**Figure 15.** Moment and Number of Bolts Relationship.**Figure 16.** Rotation and Number of Bolts Relationship.

The results of the research, as shown in **Figure 15**, show that the number of bolts has a significant effect on the beam-to-column joint, namely the non-linear moment capacity increases. The cross-sectional area of the bolt has a significant effect, so that bolts with a diameter of 12mm have a much higher moment capacity than bolts with a diameter of 10mm and 8mm. Likewise, the impact on stiffness behavior, which is rotational. The results of the research, as shown in **Figure 16**, show that the number of bolts has a significant effect on the beam-to-column joint, namely the non-linear rotational capacity increases. The

cross-sectional area of the bolt has a significant effect, so that bolts with a diameter of 12mm have a much higher rotational capacity than bolts with a diameter of 10mm and 8mm.

Table 5 show the results of the research, which is the bilinear moment-rotational relationship curve model. The calculation results show that the rotational moment capacity increases due to the influence of bolt diameter size and number of bolts. An empirical equation can be prepared by using multiple regression analysis to obtain a prediction of moment-rotational stiffness parameters, in the form of an empirical equation of the relationship between the influence of the number and diameter of bolts on the moment and rotation of the joint, as shown in Equations 8 to 11 and **Figure 17** as follows:

$$M_y = -960 + 276n_b + 79.3d_b \quad ; R^2 = 0.86 \quad (8)$$

$$M_u = -1065 + 348.6n_b + 131.9d_b \quad ; R^2 = 0.89 \quad (9)$$

$$\theta_y = -0.0251 + 0.00317n_b + 0.00283d_b \quad ; R^2 = 0.87 \quad (10)$$

$$\theta_u = -0.1174 + 0.00367n_b + 0.00275d_b \quad ; R^2 = 0.34 \quad (11)$$

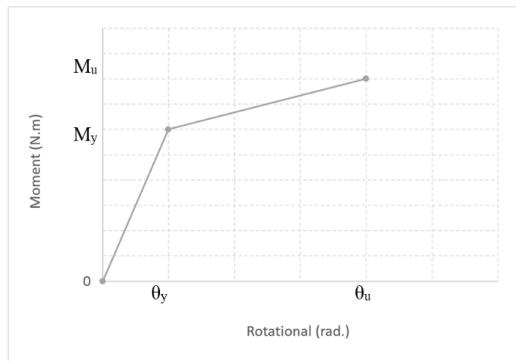


Figure 17. A Proposed Moment-Rotational Stiffness for Beam-To-Column Red Meranti (*Shorea* spp.) Timber Joints.

Equations 8 to 11 and the proposed bilinear moment-rotational model as shown in **Figure 17** can be used in the design of the moment-rotational stiffness of the beam-to-column red meranti (*Shorea* spp.) timber joints. The results of this research are the proposed empirical value of M_y , M_u , θ_y has a high R-square or R^2 value of more than 0.8. While for the θ_u parameter, has a low R^2 value of 0.34. R^2 is a measure of how well a regression model explains the variation in the dependent variable. An R-square is a

number that ranges from 0 to 1, 0 means the model doesn't explain any of the variation in the dependent variable. 1 means the model perfectly explains all the variation in the dependent variable. This trend shows that the moment capacity of the beam-to-column joint can be predicted well using these proposed empirical equations.

Modeling and analysis of 3-dimensional wooden structure systems with frame types is generally carried out using numerical method-based software. Numerical methods are commonly used to predict the behavior of structural components, connections or joints, and the structure as a whole, with the aim of obtaining efficient design results^[38,39]. One aspect of modeling and numerical testing of wooden frames is the connection stiffness parameter^[40]. Likewise, for wooden structures with a combination of frame systems and infill walls, connection stiffness is also one aspect that must be considered^[41].

However, this research used a limited number of specimens for each connection variation. Things that need to be considered are the type of red Meranti wood, the tensile strength of the steel plate as a connecting plate, and the tensile strength of the bolts in this research using certain standards based on the results of mechanical property tests. Using only one specimen per configuration is a limitation that affects statistical reliability.

5. Conclusions

Results obtained from this research propose an empirical equation to predict the moment capacity for red Meranti (*Shorea* spp.) timber joints with variations in bolt diameter size and number of bolts, namely M_y with R^2 of 0.86 and M_u with R^2 of 0.89. These results indicate a strong relationship between moment capacity, bolt diameter size, and number of bolt variables in a statistical model. The empirical equation to calculate the rotational stiffness at yield conditions (θ_y) has an R^2 of 0.87, while at ultimate conditions (θ_u) it has a very low R^2 of 0.34. In the design context, the parameters used are at elastic limit range conditions, so that the M_y and θ_y parameters can be used because these two parameters have very high R^2 values.

Joint connections with bolted fittings provide the effect of ductile behavior. The ductile beam-to-column joint connection model is suitable for use in earthquake-resistant multi-storey wooden buildings. The results obtained from

this research, which are the proposed bilinear moment-rotational stiffness relationship curve model for beam-to-column red meranti (*Shorea* spp.) timber joints, can provide benefits in modeling and analyzing the structure of multi-storey wooden buildings, especially in modeling parameters of spring element for beam-to-column joint connections of red meranti (*Shorea* spp.) timber. The results of the research show that the number of bolts has a significant effect on the beam-to-column joint, namely the non-linear moment and rotational capacity increases. The cross-sectional area of the bolt has a significant effect, so that bolts with a diameter of 12mm have a much higher moment and rotational capacities than bolts with a diameter of 10mm and 8mm.

The results of the empirical equation proposed in this study still have limitations, namely the potential for variability. For further research in the future, it is recommended to use a larger number of specimens. Research on different wood species also needs to be conducted to investigate the behavior of the wood joints.

Author Contributions

Conceptualization, Y.A.P.; methodology, Y.A.P.; validation, O.C.P.; writing—original draft preparation, Y.A.P.; writing—review and editing, Y.A.P., A.S.; visualization, O.C.P.; supervision, A.S.; project administration, O.C.P. All authors have read and agreed to the published version of the manuscript.

Funding

This work was supported by the Ministry of Education, Culture, Research, and Technology for providing funds, Regular Fundamental Research National Competitive Research, fiscal year of 2024, grant number [106/E5/PG.02.00.PL/2024].

Institutional Review Board Statement

Not applicable.

Informed Consent Statement

Not applicable.

Data Availability Statement

This research was funded by the Ministry of Education, Culture, Research, and Technology for providing funds, Regular Fundamental Research National Competitive Research. “Data is unavailable due to privacy or ethical restrictions.”

Acknowledgments

The authors are grateful for the financial support towards this research by the Ministry of Education, Culture, Research, and Technology for providing funds, Regular Fundamental Research National Competitive Research, Main Contract Number 106/E5/PG.02.00.PL/2024, fiscal year of 2024. The authors also gratefully acknowledge the support from all staffs of Structures and Concrete Laboratory of Universitas Kristen Maranatha to gain successful experimental tests results.

Conflicts of Interest

The authors declare no conflict of interest. The funders had no role in the design of the study; in the collection, analyses, or interpretation of data; in the writing of the manuscript; or in the decision to publish the results.

References

- [1] Albatici, R., Gadotti, A., Rossa, G., et al., 2017. Comparison of thermal comfort conditions in multi-storey timber frame and cross-laminated residential buildings. *Journal of Sustainable Architecture and Civil Engineering*. 2(19), 40–48. DOI: <https://doi.org/10.5755/j01.sace.19.2.17531>
- [2] Jimenez, B., Pela, L., 2023. Numerical modelling of traditional buildings composed of timber frames and masonry walls under seismic loading. *International Journal of Architectural Heritage*. 17(8), 1256–1289. DOI: <https://doi.org/10.1080/15583058.2022.2033885>
- [3] Tulebekova, S., Malo, K.A., Ronnquist, A., et al., 2022. Modeling stiffness of connections and non-structural elements for dynamic response of taller glulam timber frame buildings. *Engineering Structures*. 261, 114209. DOI: <https://doi.org/10.1016/j.engstruct.2022.114209>
- [4] Malesza, J., 2017. Effective model for analysis of wood-framed timber structures. *Archives of Civil Engineering*. 63(2), 99–112. DOI: <https://doi.org/10.1515/ace-2017-0019>

- [5] Johanides, M., Mikolasek, D., Lokaj, A., et al., 2021. Rotational stiffness and carrying capacity of timber frame corners with dowel type connections. *Materials*. 14(23), 7429. DOI: <https://doi.org/10.3390/ma14237429>
- [6] Wistara, N.J., Sukowati, M., Pamoengkas, P., 2016. The properties of red meranti wood (*Shorea leprosula* Miq) from stand with thinning and shade free gap treatments. *Journal of the Indian Academy of Wood Science*. 13(1), 21–32. DOI: <https://doi.org/10.1007/s13196-016-0161-y>
- [7] Sanjaya, F., Hadi, Y.S., Yusuf, S., 2012. Natural resistance of red meranti (*Shorea sp.*) from natural forest and plantation forest against subterranean termite (*Coptotermes curvignathus* Holmgren) [Undergraduate Thesis]. Faculty of Forestry and Environment, IPB University: Bogor, Indonesia.
- [8] Chang, W.S., Hsu, M.F., Komatsu, K., 2006. Rotational performance of traditional Nuki joints with gap I: theory and verification. *Journal of Wood Science*. 52, 58–62. DOI: <https://doi.org/10.1007/s10086-005-0734-7>
- [9] Chang, W.S., Hsu, M.F., 2007. Rotational performance of traditional Nuki joints with gap II: the behavior of butted Nuki joint and its comparison with continuous Nuki joint. *Journal of Wood Science*. 53, 401–407. DOI: <https://doi.org/10.1007/s10086-007-0880-1>
- [10] Chang, W.S., Hsu, M.F., 2010. Full-scale experiment on reinforced Taiwanese traditional timber frames. *Proceedings of the 11th World Conference on Timber Engineering*; 20–24 June 2010; Trentino, Italy. pp. 1–8.
- [11] Georgescu, S., Bedeleian, B., 2017. Effect of heat treatment on compressive and tensile strength of end to edge butt joint. *Pro Ligno*. 13(4), 500–507.
- [12] Iovane, G., Faggiano, B., 2021. Timber beam-to-column joint with steel link: design and mechanical characterization through numerical investigation. *Proceedings of the 8th International Conference on Computational Methods in Structural Dynamics and Earthquake Engineering*; 28–30 June 2021; Greece. *Eccomas Procedia*. pp. 2359–2365.
- [13] Iovane, G., Oliva, V., Faggiano, B., 2023. Design and analysis of dissipative seismic resistant heavy timber frame structures equipped with steel links. *Procedia Structural Integrity XIX Anidis Conference Seismic Engineering in Italy*. 44, 1864–1869.
- [14] Iovane, G., Rodrigues, L., Branco, J., et al., 2023. Monotonic tests on beam-to-column joint with steel link for timber seismic resistant structures. *Proceedings of the World Conference on Timber Engineering 2023 (WCTE 2023)*; 19–22 June 2023; Oslo, Norway. pp. 2173–2178. DOI: <https://doi.org/10.52202/069179-0288>
- [15] Iovane, G., Rodrigues, L., Branco, J., et al., 2023. A proposal for the mechanical classification of beam to-column joints for timber structures. *Proceedings of the World Conference on Timber Engineering 2023 (WCTE 2023)*; 19–22 June 2023; Oslo, Norway. pp. 2995–3000.
- [16] Nakatani, M., Mori, T., Komatsu, K., 2008. Study on the beam-column joint of timber frame structures using lagscrewbolts and special connectors [in Japanese]. *Journal of Structural and Construction Engineering*. 73(626), 599–606. DOI: <https://doi.org/10.3130/aijs.73.599>
- [17] Li, Z., Kitamori, A., Zhang, X., et al., 2024. Analytical investigation on the rotational behavior of dovetail mortise–tenon joints between beams and columns in traditional Chinese timber frames. *Journal of Wood Science*. 70(1), 50. DOI: <https://doi.org/10.1186/s10086-024-02162-0>
- [18] Valdes, M.D., Bohorquez, M.G., 2023. Novel Proposal of bio-based sewing timber joint: learning from diatoms. *Journal of Building Material Science*. 5(1), 1–8. DOI: <https://doi.org/10.30564/jbms.v5i1.5299>
- [19] Johanides, M., Lokaj, A., Mikolasek, D., et al., 2023. Experimental analysis of the rotational stiffness of a wooden pin-type semi-rigid connection [in Czech]. *KONSTRUKCE*. 4. Available from: <https://www.scia.net/en/news/experimental-analysis-rotational-stiffness-wooden-pin-type-semi-rigid-connection> (cited 10 December 2024).
- [20] Mirzabagheri, S., Salem, O., 2024. Numerical study of GFRP-reinforced concrete beams with straight and hooked-end bar lap splices. *Journal of Building Material Science*. 6(1), 1–16. DOI: <https://doi.org/10.30564/jbms.v6i1.6170>
- [21] Hibbeler, R.C., 2023. *Mechanics of materials*, 11th ed. Pearson: New York, USA.
- [22] Commonwealth Scientific and Industrial Research Organization, 1996. *Timber evaluation of mechanical joint systems Part 3. Earthquake loading*. Commonwealth Scientific and Industrial Research Organization: Canberra, Australia.
- [23] Sinharay, S., 2010. An overview of statistics in education. In: Peterson, P., Baker, E., McGaw, B. (eds.). *International Encyclopedia of Education*, 3rd ed. Elsevier Ltd.: Oxford, England, UK. pp. 1–11. DOI: <https://doi.org/10.1016/B978-0-08-044894-7.01719-X>
- [24] Siegel, A.F., Wagner, M.R., 2022. Multiple regression: predicting one variable from several others. In: Siegel, A.F., Wagner, M.R. (eds.). *Practical Business Statistics*, 8th ed. Academic Press: New York, USA. pp. 371–431. DOI: <https://doi.org/10.1016/B978-0-12-820025-4.00012-9>
- [25] SNI 7973-2013. 2013. *Design specifications for wood construction* [in Indonesian]. National Standardization Agency: Indonesia.

- [26] American Institute of Steel Construction, 2025. Bolt installation. Available from: <https://www.aisc.org/steel-solutions-center/engineering-faqs/6.5.-bolt-installation> (cited 10 December 2024).
- [27] ASTM E8/E8M-22. 2022. Standard test methods for tension testing of metallic materials. ASTM International: West Conshohocken, United States.
- [28] ASTM F606/F606M-19. 2019. Standard test methods for determining the mechanical properties of externally and internally threaded fasteners, washers, direct tension indicators, and rivets. ASTM International: West Conshohocken, United States.
- [29] Pranata, Y.A., 2011. Flexural behavior of Indonesian timber bolt-laminated beams [Ph.D Dissertation] [in Indonesian]. Parahyangan Catholic University: Bandung, Indonesia.
- [30] Herawati, E., Sadiyo, S., Nugroho, N., et al., 2017. Flexural yield strength characteristics of iron bolts with several bolt diameter variations [in Indonesian]. *Jurnal Teknik Sipil*. 24(3), 217–222. DOI: <https://doi.org/10.5614/jts.2017.24.3.4>
- [31] ASTM A307-21. 2021. Standard specification for carbon steel bolts, studs, and threaded rod 60 000 psi tensile strength. ASTM International: West Conshohocken, United States.
- [32] Hung Ta, 2008. HT-9501 Electro-hydraulic servo universal testing machines. Hung Ta Instrument Co. Ltd.: Thailand
- [33] Pranata, Y.A., Suryoatmono, B., 2024. Experimental tests of red meranti (*shorea* spp.) dowel bearing strength at an angle to the grain. *Wood Research*. 69(3), 369–375. DOI: <https://doi.org/10.37763/wr.1336-4561/69.3.369375>
- [34] Reboucas, A.S., Mehdipour, Z., Branco, J.M., et al., 2022. Ductile moment-resisting timber connections: a review. *Buildings*. 12(2), 240. DOI: <https://doi.org/10.3390/buildings12020240>
- [35] Park, R., 1988. Ductility evaluation from laboratory and analytical testing. *Proceedings of the 9th World Conference on Earthquake Engineering*; 2 August 1988; Tokyo–Kyoto, Japan. 8, pp. 605–616.
- [36] EN 1998-1:2004. 2004. Eurocode 8: Design of structures for earthquake resistance - part 1: general rules, seismic actions and rules for buildings. European Committee for Standardization: Brussels, Belgium.
- [37] 2024 NDS. 2024. The 2024 national design specification for wood construction. American Wood Council Wood Design Standards Committee: United States of America.
- [38] Zhu, C., 2024. Topology optimization of finite periodic structures with compliance and frequency criteria. *Journal of Metallic Material Research*. 7(1), 22–31. DOI: <https://doi.org/10.30564/jmmr.v7i1.7152>
- [39] Abdelhak, M., Belabed, Z., Tounsi, A., et al., 2023. Assessment of new quasi-3d finite element model for free vibration and stability behaviors of thick functionally graded beams. *Journal of Vibration Engineering and Technologies*. 12(2), 2231–2247. DOI: <https://doi.org/10.1007/s42417-023-00976-8>
- [40] Mikolasek, D., Marcalikova, Z., Johanides, M., et al., 2023. The aspects of numerical modelling and testing of timber frame corner with dowel type connections. *AIP Conference Proceedings*. 2950(1), 020026. DOI: <https://doi.org/10.1063/5.0184347>
- [41] Champagne, F.V., Grange, S., Sieffert, Y., et al., 2014. Numerical analysis of timber-frame structures with infill under seismic loading. *Proceedings of the World Conference on Timber Engineering 2014 (WCTE 2014)*; 10–14 August 2014; Quebec, Canada. pp. 1912–1919.